

UT-13-06  
March, 2013

# Stau with Large Mass Difference and Enhancement of $h \rightarrow \gamma\gamma$ Decay Rate in the MSSM

Teppei Kitahara<sup>†</sup> and Takahiro Yoshinaga<sup>‡</sup>

*Department of Physics, The University of Tokyo,  
Tokyo 113-0033, Japan*

## Abstract

The ATLAS and the CMS collaborations have presented results which show an excess of the  $h \rightarrow \gamma\gamma$  decay channel. In the Minimal Supersymmetric Standard Model (MSSM), this situation can be achieved by a light stau and a large left-right mixing of the staus. However, this parameter region is severely constrained by vacuum stability. In order to relax the vacuum meta-stability condition, we focus on the parameter region where the mass difference between the two staus is large. This region has not been considered yet. In this paper, we show that staus with a large mass difference can relax the vacuum meta-stability condition sufficiently even if the lighter stau mass  $m_{\tilde{\tau}_1}$  is kept light. We find that when the mass difference of two staus is large, the enhancement of the  $h \rightarrow \gamma\gamma$  decay rate becomes small in spite of a relaxation of the vacuum meta-stability condition. Because of this feature, an  $\mathcal{O}(70)\%$  enhancement of  $\Gamma(h \rightarrow \gamma\gamma)/\Gamma(h \rightarrow \gamma\gamma)_{\text{SM}}$  is difficult to achieve in the light stau scenario in the MSSM.

KEYWORDS: Supersymmetry, Higgs to diphoton decay rate, Vacuum stability

---

<sup>†</sup> Electronic address: kitahara@hep-th.phys.s.u-tokyo.ac.jp

<sup>‡</sup> Electronic address: t.yoshinaga@hep-th.phys.s.u-tokyo.ac.jp

# 1 Introduction

The ATLAS [1] and the CMS [2] collaborations discovered the Higgs-like particle, and measurements of the Higgs couplings to Standard Model (SM) particles have started at the LHC. Especially, the measurement of the Higgs coupling to diphoton is interesting, since the Higgs to diphoton decay process is a one-loop level process in the SM and can be significantly influenced by new physics beyond the SM. Both the ATLAS and the CMS collaborations have reported that the observed diphoton signal strength is  $1.5 - 1.8$  times larger than its SM prediction value, respectively [3, 4],

$$\begin{aligned}\mu(\gamma\gamma)_{\text{ATLAS}} &= 1.80 \pm 0.30 \text{ (stat)}_{-0.15}^{+0.21} \text{ (syst)}_{-0.14}^{+0.20} \text{ (theory)}, \\ \mu(\gamma\gamma)_{\text{CMS}} &= 1.564_{-0.419}^{+0.460}.\end{aligned}\tag{1}$$

On the other hand, the other signal strengths are in agreement with SM predictions.

Motivated by this experimental result, there is much literature about various new physics models [5–42]. Literature about model independent effective operators is also reported [43–45]. In the Minimal Supersymmetric (SUSY) Standard Model (MSSM) scenario, a light stau and a large left-right mixing of staus can appropriately enhance  $\mu(\gamma\gamma)$  [22–25]. However, it was pointed out that a light stau and a large left-right mixing of staus may suffer from vacuum instability [46–48], and found that the vacuum meta-stability condition severely constrains the Higgs to diphoton decay rate [49–51].

In order to relax the vacuum meta-stability condition, we have focused on the parameter region where the mass difference of the two staus is large. In this parameter region, the heavier stau raises the quadratic term of the scalar potential, and the vacuum meta-stability condition can be relaxed even if the lighter stau mass  $m_{\tilde{\tau}_1}$  is kept light. Thus, staus with large mass difference may be able to enhance the Higgs to diphoton decay rate. This region has not been considered in the literature [50, 51] yet. In this paper, we will analyze in detail about this region.

In addition, staus with large mass difference affect the Higgs to  $Z\gamma$  decay rate. Since  $SU(2)_L$  isospin and hypercharge differ between the left-handed stau  $\tilde{\tau}_L$  and the right-handed stau  $\tilde{\tau}_R$ , the dependence of the Higgs to  $Z\gamma$  decay rate as a function of  $\tilde{\tau}_1$  will change whether it is dominated by either the left- or right-handed stau. Therefore, staus with large mass difference may be able to affect both the Higgs to diphoton decay rate and the Higgs to  $Z\gamma$  decay rate with some correlation [52].

In this paper we analyze the Higgs to diphoton decay rate in a broad parameter region which includes stau with large mass difference in the MSSM. We do not assume any particular high-energy supersymmetry breaking structure. In addition, we show that when the mass difference of the two staus is large, the enhancement of the  $h \rightarrow \gamma\gamma$  decay decreases monotonically for effective  $\mu \tan \beta$ , in spite of a relaxation of the vacuum meta-stability condition, and that the enhancement of the Higgs to diphoton decay rate is up to 40 % when the lighter stau mass is larger than 100 GeV.

This paper is organized as follows. In section 2, we will evaluate the vacuum transition rate in a broad parameter region which includes staus with large mass difference, and show the effective  $\tan \beta$  dependence of the stability bound. In section 3, we will apply the vacuum stability condition which will be calculated in section 2 to the Higgs to diphoton decay rate. Section 4 is devoted to our conclusions and discussion.

## 2 Vacuum stability

First, we consider the scalar potential for the neutral component of the up-type Higgs,  $h_u$ , the left-handed stau,  $\tilde{L}$ , and the right-handed stau,  $\tilde{\tau}_R$ . Neglecting the potential for the down-type Higgs is a good approximation when  $\tan\beta$  and the CP-odd Higgs mass,  $M_A$  are very large. The scalar potential can be written as

$$\begin{aligned}
V = & \frac{1}{2}m_Z^2 \sin^2\beta(1+\Delta_t)h_u^2 + \left(m_{\tilde{L}}^2 + \frac{g^2 - g'^2}{4}v_2^2\right)\tilde{L}^2 + \left(m_{\tilde{\tau}_R}^2 + \frac{g'^2}{2}v_2^2\right)\tilde{\tau}_R^2 \\
& - \frac{2m_\tau}{v \cos\beta} \frac{1}{1+\Delta_\tau} \mu \tilde{L} \tilde{\tau}_R \left(v_u + \frac{h_u}{\sqrt{2}}\right) + \frac{g^2 - g'^2}{2\sqrt{2}} v_u h_u \tilde{L}^2 + \frac{g'^2}{\sqrt{2}} v_u h_u \tilde{\tau}_R^2 \\
& + \frac{m_Z^2 \sin^2\beta(1+\Delta_t)}{2\sqrt{2}v_u} h_u^3 + \frac{m_Z^2(1+\Delta_t)}{16v^2} h_u^4 + \frac{g^2 + g'^2}{8} \tilde{L}^4 + \frac{g'^2}{2} \tilde{\tau}_R^4 \\
& + \left\{ \left( \frac{m_\tau}{v \cos\beta} \frac{1}{1+\Delta_\tau} \right)^2 - \frac{1}{2}g'^2 \right\} \tilde{L}^2 \tilde{\tau}_R^2 + \frac{g^2 - g'^2}{8} h_u^2 \tilde{L}^2 + \frac{g'^2}{4} h_u^2 \tilde{\tau}_R^2, \quad (2)
\end{aligned}$$

where  $H_u^0 = v_u + h_u/\sqrt{2}$ , and  $v_u = v \sin\beta$  with  $v \simeq 174$  GeV.  $g'$  is the gauge coupling for  $U(1)_Y$  and  $g$  is the gauge coupling for  $SU(2)_L$ .  $m_{\tilde{L}}$  and  $m_{\tilde{\tau}_R}$  are soft SUSY breaking slepton masses. We take account of only two effects at one-loop order,  $\Delta_t$  and  $\Delta_\tau$ . Note that the full one-loop effect influences the vacuum stability condition in a few percent [51].

The leading log term of the one-loop corrections for top/stop loops  $\Delta_t$  is

$$\Delta_t \simeq \frac{3}{2\pi^2} \frac{y_t^4}{g^2 + g'^2} \log \frac{\sqrt{m_{t_1}^2 m_{t_2}^2}}{m_t^2}, \quad (3)$$

where  $y_t = m_t/v \sin\beta$  and  $m_t$  is the weak scale running top quark mass. When  $\Delta_t \simeq 1$ , the Higgs boson mass,  $m_h^2 \simeq (1+\Delta_t)m_Z^2 \sin^2\beta$ , is enhanced to 126 GeV.

$\Delta_\tau$  is the correction from the tau non-holomorphic Yukawa coupling, and its contribution becomes significant at large  $\tan\beta$  [53–55]. At the tree level, the tau Yukawa coupling is  $y_\tau = m_\tau/v \cos\beta$ . It is modified at the one-loop level as follows,

$$y_\tau = \frac{m_\tau}{v \cos\beta} \frac{1}{1+\Delta_\tau}. \quad (4)$$

The expression for the  $\Delta_\tau$  in the large  $\tan\beta$  region is given as follows,

$$\Delta_\tau \simeq -\mu \tan\beta \left\{ \frac{3}{32\pi^2} g^2 M_2 I(m_{\tilde{\nu}\tau}, M_2, \mu) - \frac{1}{16\pi^2} g'^2 M_1 I(m_{\tilde{\tau}1}, m_{\tilde{\tau}2}, M_1) \right\}, \quad (5)$$

where

$$I(a, b, c) = \frac{a^2 b^2 \ln(a^2/b^2) + b^2 c^2 \ln(b^2/c^2) + c^2 a^2 \ln(c^2/a^2)}{(a^2 - b^2)(b^2 - c^2)(a^2 - c^2)}. \quad (6)$$

In the above  $M_{1(2)}$  is the Bino (Wino) mass. If  $\text{sign}(\mu M_2) = +1$ , the sign of  $\Delta_\tau$  is minus and its absolute value is  $\mathcal{O}(0.1) - \mathcal{O}(0.2)$  in the large  $\tan\beta$  region. Note that

since, if  $y_\tau \mu$  is held constant,  $\Delta_\tau$  contribution raises the scalar potential (2) through the stau quartic term,  $\tilde{L}^2 \tilde{\tau}_R^2$ , it can relax vacuum stability [51].

Let us define  $\tan \beta_{\text{eff}}$  as follows,

$$\tan \beta_{\text{eff}} \equiv \tan \beta \frac{1}{1 + \Delta_\tau}. \quad (7)$$

Then, the tau Yukawa coupling is simplified at large  $\tan \beta$ ,

$$y_\tau \simeq \frac{m_\tau}{v} \tan \beta_{\text{eff}}. \quad (8)$$

Since  $\Delta_\tau$  is dependent on many SUSY parameters, an analysis becomes complicated. For simplicity, in the rest of this paper we treat  $\tan \beta_{\text{eff}}$  as an input parameter in the tau sector instead of considering  $\Delta_\tau$ .

The scalar potential (2) has some local minima, and the ordinary electroweak-breaking minimum is  $h_u = \tilde{L} = \tilde{\tau}_R = 0$  GeV vacuum. As the large left-right mixing of staus, i.e. large  $\mu \tan \beta_{\text{eff}}$ , the new charge-breaking minimum which leads to the  $\tilde{L} \neq 0$  or  $\tilde{\tau}_R \neq 0$  vacuum develops. Then, the minimum becomes lower than the ordinary electroweak-breaking minimum. Eventually, the electroweak-breaking vacuum (false vacuum) causes vacuum decay to the charge-breaking vacuum (true vacuum) by quantum tunneling effects.

The vacuum transition rate from the false vacuum to the true vacuum can be evaluated by semiclassical technique [56, 57]. The vacuum transition rate per unit space-time volume is evaluated as follows,

$$\frac{\Gamma}{V} = A e^{-B}, \quad (9)$$

where the prefactor  $A$  is the fourth power of the typical energy scale in the potential, and expected to be roughly  $(100 \text{ GeV})^4$ .  $B$  is the Euclidean action which is evaluated on the bounce solution. When the vacuum transition rate per unit volume  $\Gamma/V$  is smaller than the fourth power of the current value of the Hubble parameter  $H_0 \simeq 1.5 \times 10^{-42}$  GeV, i.e. the lifetime of the false vacuum is longer than the age of the universe, the false vacuum becomes meta-stable. Then the vacuum meta-stability condition is approximately given as  $B \gtrsim 400$ <sup>1</sup>.

We analyzed numerically the Euclidean action  $B$  at zero temperature by **CosmoTransitions 1.0.2** [58], which is the numerical package to analyze zero and finite temperature cosmological phase transitions for single and multiple scalar fields<sup>2</sup>. In Figure 1, we show the upper bounds on  $\mu \tan \beta_{\text{eff}}$  which satisfy  $B \geq 400$  and contours of the lighter stau mass in  $m_{\tilde{L}} - m_{\tilde{\tau}_R}$  plane for  $A_\tau = 0$  GeV,  $\tan \beta_{\text{eff}} = 70$ ,  $m_h = 126$  GeV. The solid lines are the upper bounds on  $\mu \tan \beta_{\text{eff}}$ , and the blue dashed lines are

<sup>1</sup>This meta-stability condition has only logarithmic dependence of the Hubble parameter  $H_0$  and the prefactor  $A$ . So, even if the value of  $H_0$  or  $A$  changes  $\mathcal{O}(10)\%$ , the change of this condition is less than one percent.

<sup>2</sup>In order to evaluate the bounce solution and the Euclidean action  $B$  numerically, we applied modules **tunneling1D.py** and **pathDeformation.py**. In order to evaluate them at zero temperature, we set the parameter  $\alpha = 3$  in the modules.

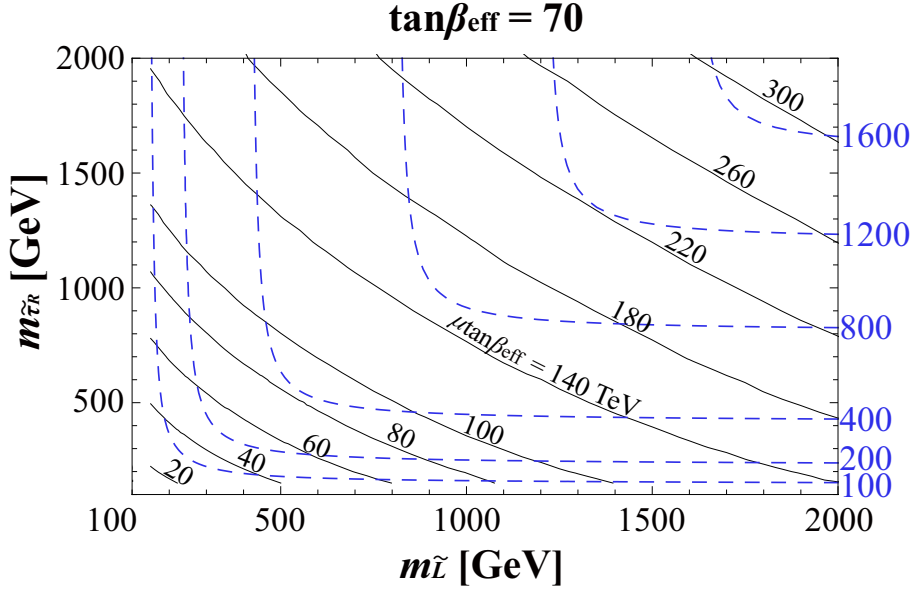


**Figure 1:** The solid lines are contours of the upper bound on  $\mu \tan \beta_{\text{eff}}$  which satisfy  $B \geq 400$  in  $m_{\tilde{L}} - m_{\tilde{R}}$  plane. The blue dashed lines are contours of the lighter stau mass  $m_{\tilde{\tau}_1}$ , where  $\mu \tan \beta_{\text{eff}}$  is taken to be the maximum value. We take  $A_\tau = 0$  GeV,  $\tan \beta_{\text{eff}} = 70$  and  $m_h = 126$  GeV.

contours of the  $m_{\tilde{\tau}_1}$ , where  $\mu \tan \beta_{\text{eff}}$  is taken to be the maximum value. When either  $m_{\tilde{L}}$  or  $m_{\tilde{R}}$  is large, we find that the vacuum meta-stability condition for  $\mu \tan \beta_{\text{eff}}$  is relaxed even if  $m_{\tilde{\tau}_1} = \mathcal{O}(100)$  GeV. Thus, in the case of staus with large mass deference, the upper bound of  $\mu \tan \beta_{\text{eff}}$  can be enlarged.

Let us discuss the  $\tan \beta_{\text{eff}}$  dependence of the upper bound on  $\mu \tan \beta_{\text{eff}}$ . At large  $\tan \beta_{\text{eff}}$ , the upper bound on  $\mu \tan \beta_{\text{eff}}$  is alleviated by  $\Delta_\tau$  effects [51]. In Figure 2, we show the  $\tan \beta_{\text{eff}}$  dependence of the upper bound on  $\mu \tan \beta_{\text{eff}}$  for  $A_\tau = 0$  GeV, and  $m_h = 126$  GeV, normalized by the upper bound on  $\mu \tan \beta_{\text{eff}}$  at  $\tan \beta_{\text{eff}} = 70$ . The blue lines correspond to the  $m_{\tilde{L}} = m_{\tilde{R}}$  case, and the blue solid (dashed, dotted) line represents  $m_{\tilde{L}} = m_{\tilde{R}} = 300$  (1000, 2000) GeV. On the other hand, the red lines correspond to the  $m_{\tilde{L}} \ll m_{\tilde{R}}$  case, and the red solid (dashed) line represents  $m_{\tilde{L}} = 200$  (300) GeV,  $m_{\tilde{R}} = 1500$  (2000) GeV. We showed that  $\tan \beta_{\text{eff}}$  can certainly relax the upper bound of  $\mu \tan \beta_{\text{eff}}$  that satisfies  $B \geq 400$ . We also found that the  $m_{\tilde{L}} = m_{\tilde{R}}$  cases are more sensitive to  $\tan \beta_{\text{eff}}$  than the stau with large mass difference cases. This is because, in the  $m_{\tilde{L}} = m_{\tilde{R}}$  cases the charged-breaking vacuum is  $\tilde{L} \sim \tilde{R} \neq 0$ , and this vacuum of the scalar potential is more sensitive to  $\tan \beta_{\text{eff}}$  than the latter cases. As a rough estimate, we found that when  $\tan \beta_{\text{eff}} \sim 90$ , the meta-stability condition is relaxed by about 5%, and when  $\tan \beta_{\text{eff}} \sim 20$ , the meta-stability condition is tightened by about 10%.

We applied a fit of a function of  $m_{\tilde{L}}$  and  $m_{\tilde{R}}$  to Figure 1. The vacuum meta-stability

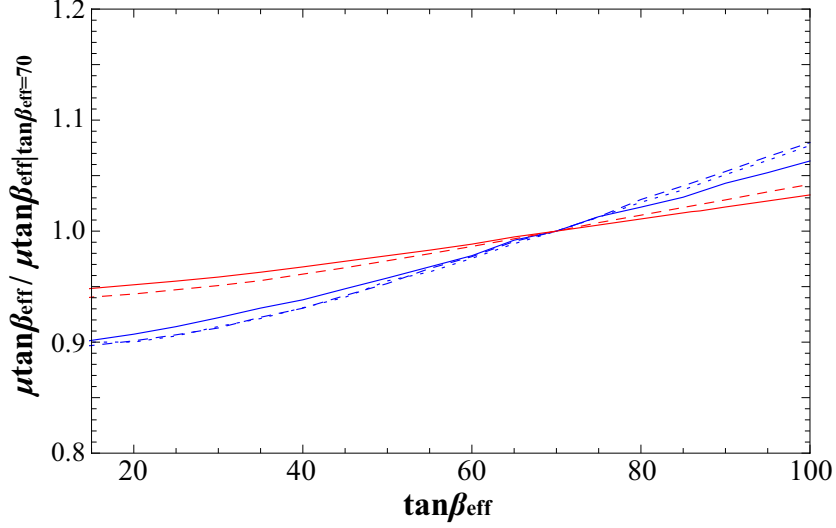


**Figure 2:**  $\tan \beta_{\text{eff}}$  dependence of the upper bound on  $\mu \tan \beta_{\text{eff}}$  that satisfies  $B \geq 400$ , normalized by the upper bound on  $\mu \tan \beta_{\text{eff}}$  at  $\tan \beta_{\text{eff}} = 70$ . We take  $A_\tau = 0$  GeV and  $m_h = 126$  GeV. The blue solid (dashed, dotted) line corresponds to  $m_{\tilde{L}} = m_{\tilde{\tau}_R} = 300$  (1000, 2000) GeV, and the red solid (dashed) line corresponds to  $m_{\tilde{L}} = 200$  (300) GeV,  $m_{\tilde{\tau}_R} = 1500$  (2000) GeV.

condition fitting formula is given by

$$|\mu \tan \beta_{\text{eff}}| < 56.9 \sqrt{m_{\tilde{L}} m_{\tilde{\tau}_R}} + 57.1 (m_{\tilde{L}} + 1.03 m_{\tilde{\tau}_R}) - 1.28 \times 10^4 \text{ GeV} \\ + \frac{1.67 \times 10^6 \text{ GeV}^2}{m_{\tilde{L}} + m_{\tilde{\tau}_R}} - 6.41 \times 10^7 \text{ GeV}^3 \left( \frac{1}{m_{\tilde{L}}^2} + \frac{0.983}{m_{\tilde{\tau}_R}^2} \right). \quad (10)$$

This formula can be applied in the region where  $m_{\tilde{L}}, m_{\tilde{\tau}_R} \leq 2$  TeV, the error of this fit being less than 1 % in this region. It is valid in the case considering not only light staus but also staus with large mass deference. Note that an asymmetry of coefficients of  $m_{\tilde{L}}$  and  $m_{\tilde{\tau}_R}$  is reflected by D-term potential, i.e.  $g'^2$  and  $g^2$  terms in Eq. (2).

Before proceeding, let us compare our results to the results of Ref. [48]. The meta-stability condition of the stau sector was evaluated numerically in the literature<sup>3</sup>. Its formula is valid in the region where both of the staus are light,  $m_{\tilde{L}}, m_{\tilde{\tau}_R} \leq 600$  GeV. We checked that our results reproduce the results of the literature in this region well, see Figure 3. We show the meta-stability bound on  $\mu \tan \beta_{\text{eff}}$  as a function of  $m_{\tilde{\tau}_R}$ . The blue lines correspond the meta-stability condition (10), and the red lines correspond meta-stability bound from Ref. [48]. We take  $m_{\tilde{L}} = 250$  GeV (solid) and  $m_{\tilde{L}} = 500$  GeV (dashed). We found that when either  $m_{\tilde{L}}$  or  $m_{\tilde{\tau}_R}$  is  $\mathcal{O}(1)$  TeV, our results deviate from

<sup>3</sup>The result of the vacuum meta-stability condition in [48] was obtained as:

$$|\mu \tan \beta| < 213.5 \sqrt{m_{\tilde{L}} m_{\tilde{\tau}_R}} - 17.0 (m_{\tilde{L}} + m_{\tilde{\tau}_R}) + 4.52 \times 10^{-2} \text{ GeV}^{-1} (m_{\tilde{L}} - m_{\tilde{\tau}_R})^2 \\ - 1.30 \times 10^4 \text{ GeV}. \quad (11)$$

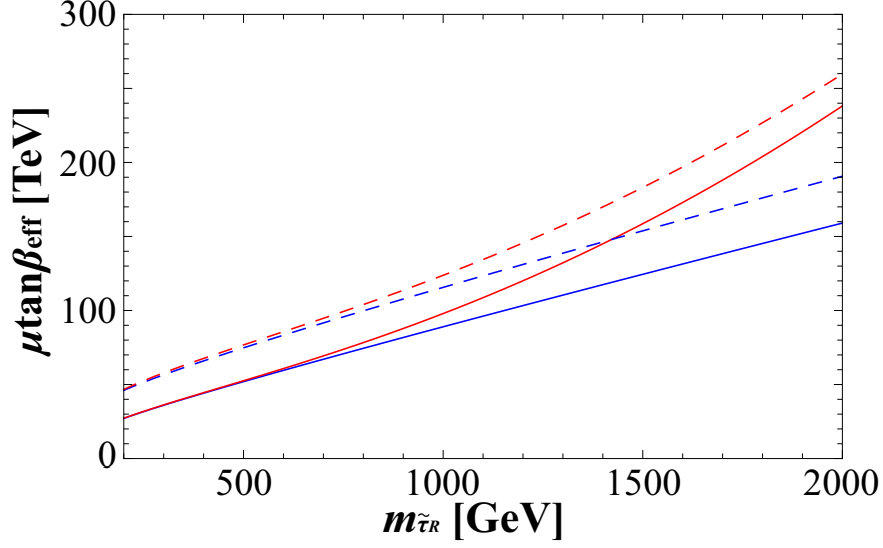


**Figure 3:** Meta-stability bound on  $\mu \tan \beta_{\text{eff}}$  as a function of  $m_{\tilde{\tau}_R}$ . The blue lines correspond the meta-stability condition (10), and the red lines correspond to the meta-stability bound from Ref. [48]. We take  $m_{\tilde{L}} = 250$  GeV (solid) and  $m_{\tilde{L}} = 500$  GeV (dashed).

the results given in the literature. We will discuss the influence of this deviation for the Higgs to diphoton decay rate in next section.

### 3 Numerical analysis

In this section, we analyze numerically the ratio of  $\Gamma(h \rightarrow \gamma\gamma)$  to its SM prediction,  $\Gamma(h \rightarrow \gamma\gamma)/\Gamma(h \rightarrow \gamma\gamma)_{SM}$ , including the parameter region of staus with large mass difference, and apply the vacuum meta-stability condition calculated in section 2 to the decay rate.

In the MSSM, an analytic expression for the Higgs to diphoton partial width is given in Refs. [59, 60],

$$\Gamma(h \rightarrow \gamma\gamma) = \frac{\alpha^2 m_h^3}{1024 \pi^3} \left| \frac{g_{hWW}}{m_W^2} A_1^h(\tau_W) + \sum_f \frac{2g_{hff}}{m_f} N_{c,f} Q_f^2 A_{\frac{1}{2}}^h(\tau_f) + A_{SUSY}^{h\gamma\gamma} \right|^2, \quad (12)$$

$$A_{SUSY}^{h\gamma\gamma} = \sum_{\tilde{f}} \frac{g_{h\tilde{f}\tilde{f}}}{m_{\tilde{f}}^2} N_{c,\tilde{f}} Q_{\tilde{f}}^2 A_0^h(\tau_{\tilde{f}}) + \sum_{i=1,2} \frac{2g_{h\chi_i^+ \chi_i^-}}{m_{\chi_i^\pm}} A_{\frac{1}{2}}^h(\tau_{\chi_i^\pm}) + \frac{g_{hH^+ H^-}}{m_{H^\pm}^2} A_0^h(\tau_{H^\pm}), \quad (13)$$

where  $\tau_i = m_h^2/4m_i^2$ ,  $m_h$  is the lightest CP-even Higgs mass,  $N_{c,i}$  is the number of colors of particle  $i$ ,  $Q_i$  is the electric charge of particle  $i$ , and the loop functions  $A_i^h(\tau)$  and the Higgs couplings  $g_{hii}$  are given in Appendix A.

In the light stau scenario, the ratio of the Higgs to diphoton partial width to its SM

prediction  $\Gamma(h \rightarrow \gamma\gamma)/\Gamma(h \rightarrow \gamma\gamma)_{SM}$  can be written in a simple formula as follows,

$$\frac{\Gamma(h \rightarrow \gamma\gamma)}{\Gamma(h \rightarrow \gamma\gamma)_{SM}} \simeq \left(1 + \sum_{i=1,2} 0.05 \frac{m_\tau \mu \tan \beta_{\text{eff}}}{m_{\tilde{\tau}_i}^2} x_L^{\tau_i} x_R^{\tau_i}\right)^2, \quad (14)$$

where the stau mass eigenstates are given by  $\tilde{\tau}_i = x_L^{\tau_i} \tilde{\tau}_L + x_R^{\tau_i} \tilde{\tau}_R$ ,  $(x_L^{\tau_i})^2 + (x_R^{\tau_i})^2 = 1$ . This simple formula implies that when the lighter stau mass  $m_{\tilde{\tau}_1}$  is kept light, a large  $\mu \tan \beta_{\text{eff}}$  can enhance the Higgs to diphoton decay rate. On the other hand, it also implies that the lighter stau  $\tilde{\tau}_1$ , which is dominantly constructed by right-handed stau  $\tilde{\tau}_R$  or left-handed stau  $\tilde{L}$  (namely,  $x_L^{\tau_1} \ll x_R^{\tau_1}$  or  $x_L^{\tau_1} \gg x_R^{\tau_1}$ ), suppresses the Higgs to diphoton decay rate. In this paper, let us call such a suppression of the Higgs to diphoton decay rate “the stau L-R mixing suppression”.

In section 2, we showed that staus with large mass difference can relax the upper bound of  $\mu \tan \beta_{\text{eff}}$ . Therefore, it may be possible to enhance the Higgs to diphoton decay rate in spite of the stau L-R mixing suppression. In order to investigate the enhancement of the Higgs to diphoton decay rate when the mass difference of the two staus is large, we apply the vacuum meta-stability condition calculated in section 2 to  $\Gamma(h \rightarrow \gamma\gamma)/\Gamma(h \rightarrow \gamma\gamma)_{SM}$ , including the parameter region of staus with large mass difference. The Higgs to diphoton decay rate in this region has not been considered yet [50, 51].

The result of our numerical computations are drawn in Figure 4 and Figure 5. In Figure 4, we show the upper bound on  $\Gamma(h \rightarrow \gamma\gamma)/\Gamma(h \rightarrow \gamma\gamma)_{SM}$  as a function of  $\mu \tan \beta_{\text{eff}}$ , when  $m_{\tilde{L}}$  and  $m_{\tilde{\tau}_R}$  are varied while keeping  $m_{\tilde{\tau}_1} = 100 \text{ GeV}^4$ . We set  $\tan \beta_{\text{eff}} = 70$ ,  $A_\tau = 0 \text{ GeV}$ ,  $m_{\tilde{Q}_3} = m_{\tilde{t}_R} = m_{\tilde{b}_R} = 2 \text{ TeV}$ ,  $A_t = 3.8 \text{ TeV}$ ,  $M_2 = 500 \text{ GeV}$ ,  $M_3 = 1.5 \text{ TeV}$  and  $M_A = 10 \text{ TeV}^5$ . The light green (yellow) region represents the  $1\sigma$  band of the observational result of the ATLAS (CMS) collaboration<sup>6</sup>. The blue solid (dashed) line represents the upper bound on  $\Gamma(h \rightarrow \gamma\gamma)/\Gamma(h \rightarrow \gamma\gamma)_{SM}$  under the vacuum meta-stability condition (10) in the case of  $m_{\tilde{L}} \leq m_{\tilde{\tau}_R}$  ( $m_{\tilde{L}} \geq m_{\tilde{\tau}_R}$ ). The red line represents the bound under the condition (11) which is given by [48]. If we do not consider the vacuum stability, the upper bound of  $\Gamma(h \rightarrow \gamma\gamma)/\Gamma(h \rightarrow \gamma\gamma)_{SM}$  is given by the dotted line.

In the low  $\mu \tan \beta_{\text{eff}}$  region,  $\mu \tan \beta_{\text{eff}} \lesssim 33 \text{ TeV}$ , there are no constraints from vacuum meta-stability, and the Higgs to diphoton decay rate is the most enhanced in the case of  $m_{\tilde{L}} \simeq m_{\tilde{\tau}_R}$  [50]. On the other hand, in the high  $\mu \tan \beta_{\text{eff}}$  region,  $\mu \tan \beta_{\text{eff}} \gtrsim 33 \text{ TeV}$ , it is constrained severely by vacuum meta-stability. In this case, the decay rate is most enhanced in the case that the mass difference of staus is non-zero, see Figure 2 in Ref. [50]. Note that there are two cases to enhance the decay rate,  $m_{\tilde{L}} \leq m_{\tilde{\tau}_R}$

<sup>4</sup>The current lower bound of the stau mass at 95 % CL is obtained by the DELPHI experiment at LEP,  $m_{\tilde{\tau}_1} > 81.9 \text{ GeV}$  [61, 62]. We take  $m_{\tilde{\tau}_1} = 100 \text{ GeV}$  as reference. When  $m_{\tilde{\tau}_1}$  is lighter, the upper bound on  $\Gamma(h \rightarrow \gamma\gamma)/\Gamma(h \rightarrow \gamma\gamma)_{SM}$  varies by  $\mathcal{O}(10) \%$

<sup>5</sup> This parameter region gives  $m_h \sim 126 \text{ GeV}$ . Moreover, large  $M_A$  ensures the validity of analyzing the vacuum meta-stability of the scalar potential in three scalar field spaces ( $h_u$ ,  $\tilde{L}$  and  $\tilde{\tau}_R$ ) [51].

<sup>6</sup>Note that the signal strength which was observed by ATLAS (CMS) is not equivalent to the ratio of the Higgs partial width to its SM prediction. For simplicity, we assume  $\sigma(pp \rightarrow h)/\sigma(pp \rightarrow h)_{SM} \times \Gamma(h \rightarrow \text{All})_{SM}/\Gamma(h \rightarrow \text{All}) = 1$  in this paper, and the signal strength becomes equivalent to the ratio of the Higgs partial width to its SM prediction,  $\mu(\gamma\gamma) = \Gamma(h \rightarrow \gamma\gamma)/\Gamma(h \rightarrow \gamma\gamma)_{SM}$ .



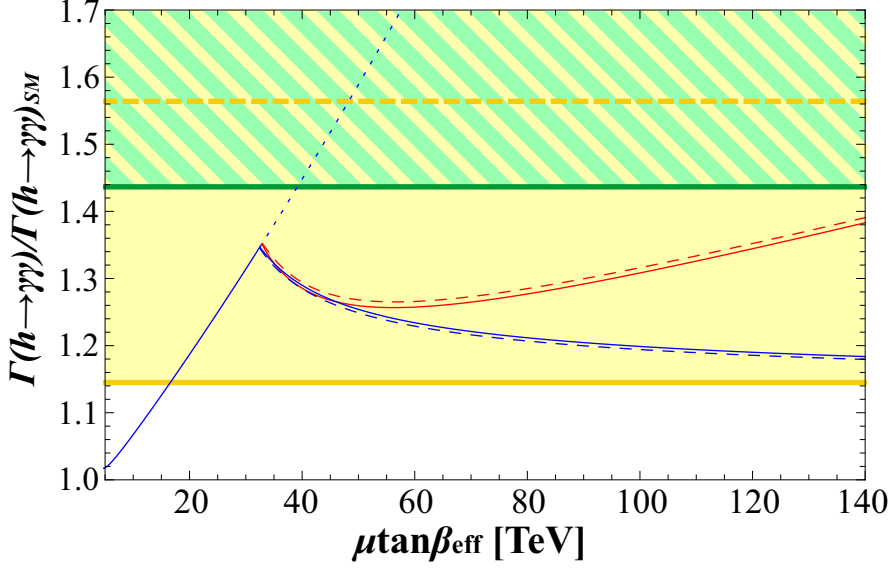


**Figure 4:** The upper bound on  $\Gamma(h \rightarrow \gamma\gamma)/\Gamma(h \rightarrow \gamma\gamma)_{\text{SM}}$  as a function of  $\mu \tan \beta_{\text{eff}}$ , when  $m_{\tilde{L}}$  and  $m_{\tilde{\tau}_R}$  are varied while keeping  $m_{\tilde{\tau}_1} = 100 \text{ GeV}$ . We set  $\tan \beta_{\text{eff}} = 70$ . The blue solid (dashed) line represents the upper bound on  $\Gamma(h \rightarrow \gamma\gamma)/\Gamma(h \rightarrow \gamma\gamma)_{\text{SM}}$  under the vacuum meta-stability condition (10) in the case of  $m_{\tilde{L}} \leq m_{\tilde{\tau}_R}$  ( $m_{\tilde{L}} \geq m_{\tilde{\tau}_R}$ ). The red line represents the bound under the condition (11) which is given by [48]. If we do not consider the vacuum stability, the upper bound of  $\Gamma(h \rightarrow \gamma\gamma)/\Gamma(h \rightarrow \gamma\gamma)_{\text{SM}}$  is given by the blue dotted line.

and  $m_{\tilde{L}} \geq m_{\tilde{\tau}_R}$ . When  $\mu \tan \beta_{\text{eff}}$  becomes larger, a larger stau mass difference is required to enhance the decay rate under the vacuum meta-stability condition, e.g. the decay rate is most enhanced in the case of  $(m_{\tilde{L}}, m_{\tilde{\tau}_R}) = (155 \text{ GeV}, 1650 \text{ GeV})$  and  $(1690 \text{ GeV}, 153 \text{ GeV})$ , when  $\mu \tan \beta_{\text{eff}} = 120 \text{ TeV}$ . As a result, we found that the upper bound on  $\Gamma(h \rightarrow \gamma\gamma)/\Gamma(h \rightarrow \gamma\gamma)_{\text{SM}}$  decreases monotonically for  $\mu \tan \beta_{\text{eff}}$  under the vacuum meta-stability condition (10). This result implies that the effect of the stau L-R mixing suppression in the Higgs to diphoton decay rate is always larger than that of the relaxation of the vacuum meta-stability. We also found that the enhancement of the Higgs to diphoton decay rate is up to 35% at  $m_{\tilde{L}} \simeq m_{\tilde{\tau}_R}$  and  $\mu \tan \beta_{\text{eff}} = 32.5 \text{ TeV}$ . This result is consistent with Ref. [51]. In addition, in the high  $\mu \tan \beta_{\text{eff}}$  region, we found that the upper bound on  $\Gamma(h \rightarrow \gamma\gamma)/\Gamma(h \rightarrow \gamma\gamma)_{\text{SM}}$  under (10) deviates significantly from the result under (11). The reason is that the vacuum meta-stability condition (11) is a fitted formula for low  $m_{\tilde{L}}$  and  $m_{\tilde{\tau}_R}$  region. When the staus experience a large mass difference, it becomes unreasonable to apply (11) as the vacuum meta-stability condition, see Figure 3.

In Figure 5, we show the upper bound on  $\Gamma(h \rightarrow \gamma\gamma)/\Gamma(h \rightarrow \gamma\gamma)_{\text{SM}}$  in the case we applied a 5%-relaxed or a 10%-severe vacuum meta-stability condition to  $\Gamma(h \rightarrow \gamma\gamma)/\Gamma(h \rightarrow \gamma\gamma)_{\text{SM}}$ . The 5%-relaxed and 10%-severe conditions represent the meta-stability condition under  $\tan \beta_{\text{eff}} \sim 90$  and  $\tan \beta_{\text{eff}} \sim 20$ , see section 2. We take the same

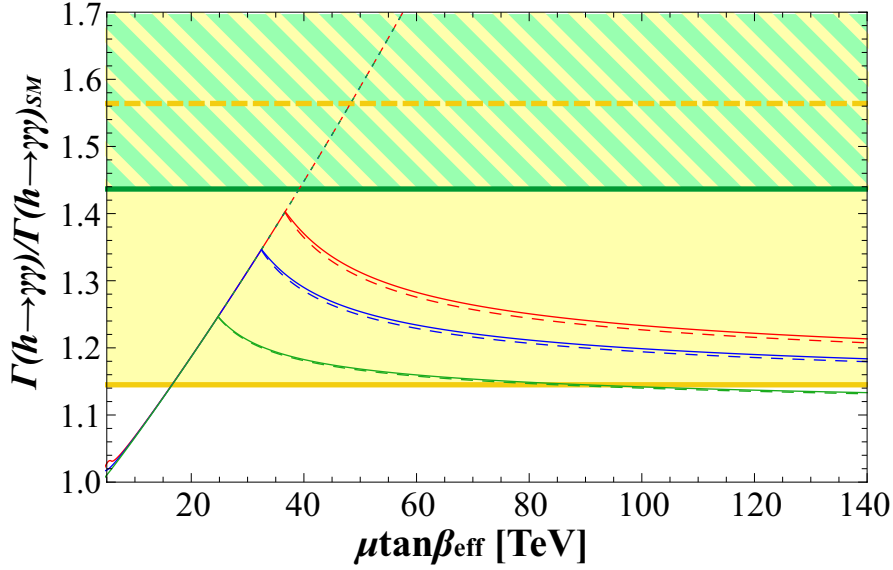


**Figure 5:** The upper bound on  $\Gamma(h \rightarrow \gamma\gamma)/\Gamma(h \rightarrow \gamma\gamma)_{\text{SM}}$  as a function of  $\mu \tan \beta_{\text{eff}}$ , when  $m_{\tilde{L}}$  and  $m_{\tilde{\tau}R}$  are varied while keeping  $m_{\tilde{\tau}1} = 100$  GeV. We set  $\tan \beta_{\text{eff}} = 70$ . The red and green lines represent the upper bound under a 5%-relaxed and a 10%-severe vacuum stability condition. All solid (dashed) lines represent the results in the case of  $m_{\tilde{L}} \leq m_{\tilde{\tau}R}$  ( $m_{\tilde{L}} \geq m_{\tilde{\tau}R}$ ). If we would not consider the vacuum stability, the upper bound of  $\Gamma(h \rightarrow \gamma\gamma)/\Gamma(h \rightarrow \gamma\gamma)_{\text{SM}}$  would be given by the dotted line.

input parameters as the case of Figure 4. The blue lines are also the same in Figure 4. The red and green lines represent the upper bound on  $\Gamma(h \rightarrow \gamma\gamma)/\Gamma(h \rightarrow \gamma\gamma)_{\text{SM}}$  under the 5%-relaxed and the 10%-severe vacuum stability condition. All solid (dashed) lines represent the results in the case of  $m_{\tilde{L}} \leq m_{\tilde{\tau}R}$  ( $m_{\tilde{L}} \geq m_{\tilde{\tau}R}$ ). The yellow and green regions are the same in Figure 4. As a result, we found that when we apply the 10%-severe and the 5%-relaxed condition to the Higgs to diphoton decay rate at  $m_{\tilde{\tau}1} = 100$  GeV, the enhancements in the decay rate are up to 25% and 40%, at  $\mu \tan \beta_{\text{eff}} = 24.8$  TeV and 36.7 TeV, respectively.

## 4 Conclusions and Discussion

The ATLAS and CMS collaborations discovered a Higgs-like particle, and the measurements of the Higgs couplings to SM particles started at the LHC. They have also presented the result of an excess in the  $h \rightarrow \gamma\gamma$  decay channel. In the MSSM, this situation can be achieved by a light stau and a large left-right mixing of staus scenario. However, this parameter region is severely constrained by vacuum stability. When the mass difference between the two staus is large, the condition can be relaxed, since the heavier stau raises the quadratic term of the scalar potential. In addition, the tau non-holomorphic Yukawa coupling also can relax the condition, and its effect

can be expressed by  $\tan\beta_{\text{eff}}$  in the stau sector.

In this paper, we evaluated the vacuum transition rate in a broad parameter region which includes the parameter region of staus with large mass difference. We found that staus with large mass difference can relax the vacuum meta-stability condition sufficiently even if the lighter stau mass  $m_{\tilde{\tau}_1}$  is kept light. Further, we got a fitting formula of the vacuum meta-stability condition as Eq. (10), and studied the  $\tan\beta_{\text{eff}}$  dependence of the condition. For example, when  $\tan\beta_{\text{eff}} \sim 20$  or  $\tan\beta_{\text{eff}} \sim 90$ , the vacuum meta-stability condition changes to a 10%-severe one or to a 5%-relaxed one.

Then, we analyzed numerically the ratio of the Higgs to diphoton decay rate to its SM prediction  $\Gamma(h \rightarrow \gamma\gamma)/\Gamma(h \rightarrow \gamma\gamma)_{\text{SM}}$ , including the parameter region of staus with large mass difference. This parameter region has not been considered yet. We found that when the mass difference of the two staus is large, the  $h \rightarrow \gamma\gamma$  decay rate decreases monotonically for  $\mu \tan\beta_{\text{eff}}$  under the vacuum meta-stability condition. This result implies that the effect of the stau L-R mixing suppression in the decay rate is always larger than the effect of the relaxation of the vacuum meta-stability condition. When  $\tan\beta_{\text{eff}} = 70$ , the enhancement of  $\Gamma(h \rightarrow \gamma\gamma)/\Gamma(h \rightarrow \gamma\gamma)_{\text{SM}}$  is up to 35% at  $\mu \tan\beta_{\text{eff}} = 32.5$  TeV in the case of  $m_{\tilde{L}} \simeq m_{\tilde{\tau}_R}$ . This results is consistent with Ref. [51]. We also found that when we apply 10%-severe vacuum condition (10), and 5%-relaxed one to the decay rate at  $m_{\tilde{\tau}_1} = 100$  GeV, the enhancement of the  $\Gamma(h \rightarrow \gamma\gamma)/\Gamma(h \rightarrow \gamma\gamma)_{\text{SM}}$  is up to 25%, and 40% at  $\mu \tan\beta_{\text{eff}} = 24.8$  TeV, and 36.7 TeV, respectively. As a result, it is found that an  $\mathcal{O}(70)\%$  enhancement of  $\Gamma(h \rightarrow \gamma\gamma)/\Gamma(h \rightarrow \gamma\gamma)_{\text{SM}}$  is difficult in the light stau scenario in the MSSM.

Furthermore, staus with large mass difference may be able to affect the Higgs to  $Z\gamma$  decay rate [52]. Since  $SU(2)_L$  isospin and hypercharge differ between the left-handed stau  $\tilde{\tau}_L$  and the right-handed stau  $\tilde{\tau}_R$ , the dependence of the Higgs to  $Z\gamma$  decay rate as a function of  $\tilde{\tau}_1$  will change whether it is dominated by the left- or right-handed stau. If it turns out that the  $Z\gamma$  signal strength is not in agreement with the SM prediction by future experiments, the light stau scenario with a large mass difference might be important.

## Acknowledgements

We are grateful to Martin Stoll for a careful reading of this paper, and Motoi Endo for useful comments and discussions. The work of T.K. was supported by Global COE Program “the Physical Sciences Frontier”, MEXT, Japan. The work of T.Y. was supported by an Advanced Leading Graduate Course for Photon Science grant.

# Appendix

## A Loop functions and Higgs couplings

### A.1 The Loop functions $A_i^h(\tau)$

$$\begin{aligned} A_1^h(\tau) &= 2 + 3\tau + 3\tau(2 - \tau)f(\tau), \\ A_{\frac{1}{2}}^h(\tau) &= -2\tau(1 + (1 - \tau)f(\tau)), \\ A_0^h(\tau) &= \tau(1 - \tau f(\tau)), \end{aligned} \quad (15)$$

where

$$f(\tau) = \begin{cases} \arcsin^2(\sqrt{\frac{1}{\tau}}), & \text{if } \tau \geq 1, \\ -\frac{1}{4} \left( \ln\left(\frac{\eta_+}{\eta_-}\right) - i\pi \right)^2, & \text{if } \tau \leq 1, \end{cases} \quad (16)$$

$$\eta_{\pm} \equiv (1 \pm \sqrt{1 - \tau}). \quad (17)$$

### A.2 The Higgs couplings in the MSSM

$$g_{hWW} = \frac{g^2 v}{\sqrt{2}} \sin(\beta - \alpha), \quad (18)$$

$$g_{hff(\text{up type})} = \frac{m_f}{\sqrt{2}v} \frac{\cos \alpha}{\sin \beta}, \quad (19)$$

$$g_{hff(\text{down type})} = \frac{m_f}{\sqrt{2}v} \frac{-\sin \alpha}{\cos \beta}, \quad (20)$$

$$\begin{aligned} g_{h\tilde{f}_i\tilde{f}_i(\text{up type})} &= \left( (-I_{3,L} + (I_{3,L} + Y_L) \sin^2 \theta_W) \frac{gm_Z}{\cos \theta_W} \sin(\alpha + \beta) + \frac{\sqrt{2}m_f^2 \cos \alpha}{v \sin \beta} \right) (x_L^{f_i})^2 \\ &+ \left( -Y_R \sin^2 \theta_W \frac{gm_Z}{\cos \theta_W} \sin(\alpha + \beta) + \frac{\sqrt{2}m_f^2 \cos \alpha}{v \sin \beta} \right) (x_R^{f_i})^2 \\ &+ \frac{\sqrt{2}m_f}{v} \frac{\mu \sin \alpha + A_f \cos \alpha}{\sin \beta} x_L^{f_i} x_R^{f_i}, \end{aligned} \quad (21)$$

$$\begin{aligned} g_{h\tilde{f}_i\tilde{f}_i(\text{down type})} &= \left( (-I_{3,L} + (I_{3,L} + Y_L) \sin^2 \theta_W) \frac{gm_Z}{\cos \theta_W} \sin(\alpha + \beta) - \frac{\sqrt{2}m_f^2 \sin \alpha}{v \cos \beta} \right) (x_L^{f_i})^2 \\ &+ \left( -Y_R \sin^2 \theta_W \frac{gm_Z}{\cos \theta_W} \sin(\alpha + \beta) - \frac{\sqrt{2}m_f^2 \sin \alpha}{v \cos \beta} \right) (x_R^{f_i})^2 \\ &- \frac{\sqrt{2}m_f}{v} \frac{\mu \cos \alpha + A_f \sin \alpha}{\cos \beta} x_L^{f_i} x_R^{f_i}, \end{aligned} \quad (22)$$

$$g_{h\chi_i^+\chi_i^-} = \frac{g}{\sqrt{2}} (-\mathbf{V}_{i1}\mathbf{U}_{i2} \sin \alpha + \mathbf{V}_{i2}\mathbf{U}_{i1} \cos \alpha), \quad (23)$$

$$g_{hH^+H^-} = g \left( m_W \sin(\beta - \alpha) + \frac{m_Z \cos 2\beta}{2 \cos \theta_W} \sin(\alpha + \beta) \right), \quad (24)$$

where  $Y_{L/R}$  and  $I_{3,L/R}$  represent hypercharge and isospin of left/right-handed sfermion, sfermion mass eigenstates represented by  $\tilde{f}_i = x_L^{f_i} \tilde{f}_L + x_R^{f_i} \tilde{f}_R$ ,  $\theta_W$  is the Weinberg angle, and  $\alpha$  is a rotation angle which translates the gauge-eigenstate basis of the CP-even Higgs mass matrix into the mass-eigenstate basis of one. The chargino mass matrix can be diagonalized to a real positive diagonal mass matrix by two  $2 \times 2$  unitary matrices  $\mathbf{U}$  and  $\mathbf{V}$  as follows,

$$\mathbf{U}^* \begin{pmatrix} M_2 & \sqrt{2}m_W \sin \beta \\ \sqrt{2}m_W \cos \beta & \mu \end{pmatrix} \mathbf{V}^\dagger = \begin{pmatrix} m_{\chi_1^\pm} & 0 \\ 0 & m_{\chi_2^\pm} \end{pmatrix}. \quad (25)$$

## References

- [1] **ATLAS** Collaboration, G. Aad *et al.*, “Observation of a new particle in the search for the Standard Model Higgs boson with the ATLAS detector at the LHC,” *Phys.Lett.* **B716** (2012) 1–29, [arXiv:1207.7214 \[hep-ex\]](#).
- [2] **CMS** Collaboration, S. Chatrchyan *et al.*, “Observation of a new boson at a mass of 125 GeV with the CMS experiment at the LHC,” *Phys.Lett.* **B716** (2012) 30–61, [arXiv:1207.7235 \[hep-ex\]](#).
- [3] **ATLAS** Collaboration, “Observation and study of the Higgs boson candidate in the two photon decay channel with the ATLAS detector at the LHC,” Tech. Rep. ATLAS-CONF-2012-168, CERN, Geneva, Dec, 2012.
- [4] **CMS** Collaboration, “Combination of standard model Higgs boson searches and measurements of the properties of the new boson with a mass near 125 GeV,” Tech. Rep. CMS-PAS-HIG-12-045, Nov, 2012.
- [5] M. Carena, I. Low, and C. E. Wagner, “Implications of a Modified Higgs to Diphoton Decay Width,” *JHEP* **1208** (2012) 060, [arXiv:1206.1082 \[hep-ph\]](#).
- [6] C.-W. Chiang and K. Yagyu, “Higgs boson decays to  $\gamma\gamma$  and  $Z\gamma$  in models with Higgs extensions,” [arXiv:1207.1065 \[hep-ph\]](#).
- [7] H. Cheon and S. K. Kang, “Constraining parameter space in type-II two-Higgs doublet model in light of a 125 GeV Higgs boson,” [arXiv:1207.1083 \[hep-ph\]](#).
- [8] M. R. Buckley and D. Hooper, “Are There Hints of Light Stops in Recent Higgs Search Results?,” [arXiv:1207.1445 \[hep-ph\]](#).
- [9] H. An, T. Liu, and L.-T. Wang, “125 GeV Higgs Boson, Enhanced Di-photon Rate, and Gauged U(1)PQ-Extended MSSM,” [arXiv:1207.2473 \[hep-ph\]](#).

- [10] A. Joglekar, P. Schwaller, and C. E. Wagner, “Dark Matter and Enhanced Higgs to Di-photon Rate from Vector-like Leptons,” [arXiv:1207.4235 \[hep-ph\]](#).
- [11] N. Arkani-Hamed, K. Blum, R. T. D’Agnolo, and J. Fan, “2:1 for Naturalness at the LHC?,” [arXiv:1207.4482 \[hep-ph\]](#).
- [12] N. Haba, K. Kaneta, Y. Mimura, and R. Takahashi, “Enhancement of Higgs to diphoton decay width in non-perturbative Higgs model,” [arXiv:1207.5102 \[hep-ph\]](#).
- [13] L. G. Almeida, E. Bertuzzo, P. A. Machado, and R. Z. Funchal, “Does  $H \rightarrow \gamma\gamma$  Taste like vanilla New Physics?,” [arXiv:1207.5254 \[hep-ph\]](#).
- [14] T. Abe, N. Chen, and H.-J. He, “LHC Higgs Signatures from Extended Electroweak Gauge Symmetry,” *JHEP* **1301** (2013) 082, [arXiv:1207.4103 \[hep-ph\]](#).
- [15] A. Delgado, G. Nardini, and M. Quiros, “Large diphoton Higgs rates from supersymmetric triplets,” [arXiv:1207.6596 \[hep-ph\]](#).
- [16] J. Kearney, A. Pierce, and N. Weiner, “Vectorlike Fermions and Higgs Couplings,” [arXiv:1207.7062 \[hep-ph\]](#).
- [17] J. R. Espinosa, C. Grojean, V. Sanz, and M. Trott, “NSUSY fits,” [arXiv:1207.7355 \[hep-ph\]](#).
- [18] I. Dorsner, S. Fajfer, A. Greljo, and J. F. Kamenik, “Higgs Uncovering Light Scalar Remnants of High Scale Matter Unification,” [arXiv:1208.1266 \[hep-ph\]](#).
- [19] K. Schmidt-Hoberg and F. Staub, “Enhanced  $h \rightarrow \gamma\gamma$  rate in MSSM singlet extensions,” [arXiv:1208.1683 \[hep-ph\]](#).
- [20] M. Reece, “Vacuum Instabilities with a Wrong-Sign Higgs-Gluon-Gluon Amplitude,” [arXiv:1208.1765 \[hep-ph\]](#).
- [21] H. Davoudiasl, H.-S. Lee, and W. J. Marciano, “Dark Side of Higgs Diphoton Decays and Muon  $g-2$ ,” [arXiv:1208.2973 \[hep-ph\]](#).
- [22] M. Carena, S. Gori, N. R. Shah, and C. E. Wagner, “A 125 GeV SM-like Higgs in the MSSM and the  $\gamma\gamma$  rate,” *JHEP* **1203** (2012) 014, [arXiv:1112.3336 \[hep-ph\]](#).
- [23] J.-J. Cao, Z.-X. Heng, J. M. Yang, Y.-M. Zhang, and J.-Y. Zhu, “A SM-like Higgs near 125 GeV in low energy SUSY: a comparative study for MSSM and NMSSM,” *JHEP* **1203** (2012) 086, [arXiv:1202.5821 \[hep-ph\]](#).
- [24] M. Carena, S. Gori, N. R. Shah, C. E. Wagner, and L.-T. Wang, “Light Stau Phenomenology and the Higgs  $\gamma\gamma$  Rate,” *JHEP* **1207** (2012) 175, [arXiv:1205.5842 \[hep-ph\]](#).

- [25] M. A. Ajaib, I. Gogoladze, and Q. Shafi, “Higgs Boson Production and Decay: Effects from Light Third Generation and Vectorlike Matter,” [arXiv:1207.7068 \[hep-ph\]](#).
- [26] N. D. Christensen, T. Han, and S. Su, “MSSM Higgs Bosons at The LHC,” *Phys.Rev.* **D85** (2012) 115018, [arXiv:1203.3207 \[hep-ph\]](#).
- [27] K. Hagiwara, J. S. Lee, and J. Nakamura, “Properties of 125 GeV Higgs boson in non-decoupling MSSM scenarios,” [arXiv:1207.0802 \[hep-ph\]](#).
- [28] R. Benbrik, M. G. Bock, S. Heinemeyer, O. Stal, G. Weiglein, *et al.*, “Confronting the MSSM and the NMSSM with the Discovery of a Signal in the two Photon Channel at the LHC,” [arXiv:1207.1096 \[hep-ph\]](#).
- [29] L. Wang and X.-F. Han, “130 GeV gamma-ray line and enhancement of  $h \rightarrow \gamma\gamma$  in the Higgs triplet model plus a scalar dark matter,” *Phys.Rev.* **D87** (2013) 015015, [arXiv:1209.0376 \[hep-ph\]](#).
- [30] E. J. Chun, H. M. Lee, and P. Sharma, “Vacuum Stability, Perturbativity, EWPD and Higgs-to-diphoton rate in Type II Seesaw Models,” *JHEP* **1211** (2012) 106, [arXiv:1209.1303 \[hep-ph\]](#).
- [31] I. Picek and B. Radovic, “Enhancement of  $h \rightarrow \gamma\gamma$  by seesaw-motivated exotic scalars,” *Phys.Lett.* **B719** (2013) 404–408, [arXiv:1210.6449 \[hep-ph\]](#).
- [32] K. Choi, S. H. Im, K. S. Jeong, and M. Yamaguchi, “Higgs mixing and diphoton rate enhancement in NMSSM models,” *JHEP* **1302** (2013) 090, [arXiv:1211.0875 \[hep-ph\]](#).
- [33] K. Schmidt-Hoberg, F. Staub, and M. W. Winkler, “Enhanced diphoton rates at Fermi and the LHC,” *JHEP* **1301** (2013) 124, [arXiv:1211.2835 \[hep-ph\]](#).
- [34] W. Chao, J.-H. Zhang, and Y. Zhang, “Vacuum Stability and Higgs Diphoton Decay Rate in the Zee-Babu Model,” [arXiv:1212.6272 \[hep-ph\]](#).
- [35] W.-F. Chang, J. N. Ng, and J. M. Wu, “Constraints on New Scalars from the LHC 125 GeV Higgs Signal,” *Phys.Rev.* **D86** (2012) 033003, [arXiv:1206.5047 \[hep-ph\]](#).
- [36] E. Bertuzzo, P. A. Machado, and R. Zukanovich Funchal, “Can New Colored Particles Illuminate the Higgs?,” *JHEP* **1302** (2013) 086, [arXiv:1209.6359 \[hep-ph\]](#).
- [37] L. Basso and F. Staub, “Enhancing  $h \rightarrow \gamma\gamma$  with staus in SUSY models with extended gauge sector,” *Phys.Rev.* **D87** (2013) 015011, [arXiv:1210.7946 \[hep-ph\]](#).
- [38] M. Aoki, S. Kanemura, M. Kikuchi, and K. Yagyu, “Radiative corrections to the Higgs boson couplings in the triplet model,” *Phys.Rev.* **D87** (2013) 015012, [arXiv:1211.6029 \[hep-ph\]](#).

- [39] L. Basso, O. Fischer, and J. van der Bij, “A singlet-triplet extension for the Higgs search at LEP and LHC,” [arXiv:1212.5560](#) [[hep-ph](#)].
- [40] S. Funatsu, H. Hatanaka, Y. Hosotani, Y. Orikasa, and T. Shimotani, “Novel universality and Higgs decay  $H \rightarrow \gamma\gamma$ , gg in the  $SO(5) \times U(1)$  gauge-Higgs unification,” [arXiv:1301.1744](#) [[hep-ph](#)].
- [41] F. Goertz, U. Haisch, and M. Neubert, “Bounds on Warped Extra Dimensions from a Standard Model-like Higgs Boson,” *Phys.Lett.* **B713** (2012) 23–28, [arXiv:1112.5099](#) [[hep-ph](#)].
- [42] A. Carmona and F. Goertz, “Custodial Leptons and Higgs Decays,” [arXiv:1301.5856](#) [[hep-ph](#)].
- [43] M. Berg, I. Buchberger, D. Ghilencea, and C. Petersson, “Higgs diphoton rate enhancement from supersymmetric physics beyond the MSSM,” [arXiv:1212.5009](#) [[hep-ph](#)].
- [44] C. Grojean, E. E. Jenkins, A. V. Manohar, and M. Trott, “Renormalization Group Scaling of Higgs Operators and  $\Gamma(h \rightarrow \gamma\gamma)$ ,” [arXiv:1301.2588](#) [[hep-ph](#)].
- [45] J. Elias-Miro, J. Espinosa, E. Masso, and A. Pomarol, “Renormalization of dimension-six operators relevant for the Higgs decay  $h \rightarrow \gamma\gamma$ ,” [arXiv:1302.5661](#) [[hep-ph](#)].
- [46] J. Casas, A. Lleyda, and C. Munoz, “Strong constraints on the parameter space of the MSSM from charge and color breaking minima,” *Nucl.Phys.* **B471** (1996) 3–58, [arXiv:hep-ph/9507294](#) [[hep-ph](#)].
- [47] R. Rattazzi and U. Sarid, “Large tan Beta in gauge mediated SUSY breaking models,” *Nucl.Phys.* **B501** (1997) 297–331, [arXiv:hep-ph/9612464](#) [[hep-ph](#)].
- [48] J. Hisano and S. Sugiyama, “Charge-breaking constraints on left-right mixing of stau’s,” *Phys.Lett.* **B696**, **B719** (2011, 2013) 92–96, [arXiv:1011.0260](#) [[hep-ph](#)].
- [49] R. Sato, K. Tobioka, and N. Yokozaki, “Enhanced Diphoton Signal of the Higgs Boson and the Muon g-2 in Gauge Mediation Models,” *Phys.Lett.* **B716** (2012) 441–445, [arXiv:1208.2630](#) [[hep-ph](#)].
- [50] T. Kitahara, “Vacuum Stability Constraints on the Enhancement of the  $h \rightarrow \gamma\gamma$  rate in the MSSM,” *JHEP* **1211** (2012) 021, [arXiv:1208.4792](#) [[hep-ph](#)].
- [51] M. Carena, S. Gori, I. Low, N. R. Shah, and C. E. Wagner, “Vacuum Stability and Higgs Diphoton Decays in the MSSM,” *JHEP* **1302** (2013) 114, [arXiv:1211.6136](#) [[hep-ph](#)].
- [52] T. Kitahara and T. Yoshinaga, work in progress.



- [53] M. S. Carena, M. Olechowski, S. Pokorski, and C. Wagner, “Electroweak symmetry breaking and bottom - top Yukawa unification,” *Nucl.Phys.* **B426** (1994) 269–300, [arXiv:hep-ph/9402253](#) [hep-ph].
- [54] D. M. Pierce, J. A. Bagger, K. T. Matchev, and R.-j. Zhang, “Precision corrections in the minimal supersymmetric standard model,” *Nucl.Phys.* **B491** (1997) 3–67, [arXiv:hep-ph/9606211](#) [hep-ph].
- [55] J. Guasch, W. Hollik, and S. Penaranda, “Distinguishing Higgs models in  $H \rightarrow b \text{ anti-}b / H \rightarrow \tau^+ \tau^-$ ,” *Phys.Lett.* **B515** (2001) 367–374, [arXiv:hep-ph/0106027](#) [hep-ph].
- [56] S. R. Coleman, “The Fate of the False Vacuum. 1. Semiclassical Theory,” *Phys.Rev.* **D15** (1977) 2929–2936.
- [57] J. Callan, Curtis G. and S. R. Coleman, “The Fate of the False Vacuum. 2. First Quantum Corrections,” *Phys.Rev.* **D16** (1977) 1762–1768.
- [58] C. L. Wainwright, “CosmoTransitions: Computing Cosmological Phase Transition Temperatures and Bubble Profiles with Multiple Fields,” *Comput.Phys.Commun.* **183** (2012) 2006–2013, [arXiv:1109.4189](#) [hep-ph].
- [59] M. A. Shifman, A. Vainshtein, M. Voloshin, and V. I. Zakharov, “Low-Energy Theorems for Higgs Boson Couplings to Photons,” *Sov.J.Nucl.Phys.* **30** (1979) 711–716.
- [60] G. K. S. D. John F. Gunion, Howard E. Haber, *The Higgs hunter’s guide*. Westview Press, 1990.
- [61] **DELPHI Collaboration** Collaboration, J. Abdallah *et al.*, “Searches for supersymmetric particles in  $e^+ e^-$  collisions up to 208-GeV and interpretation of the results within the MSSM,” *Eur.Phys.J.* **C31** (2003) 421–479, [arXiv:hep-ex/0311019](#) [hep-ex].
- [62] **Particle Data Group** Collaboration, J. Beringer *et al.*, “Review of Particle Physics (RPP),” *Phys.Rev.* **D86** (2012) 010001.